Carbon-based nanomaterials in electromagnetic interference shielding: graphene oxide, reduced graphene oxide, electrochemically exfoliated graphene, and biomass-derivated graphene

S. Jovanovic, M. Yasir, W. Saeed, I. Spanopoulos, Z. Syrgiannis, M. Milenkovic, D. Kepic

***Abstract*—Graphene is one of the emerging materials. Its astonishing properties have attracted tremendous attention from various fields, such as medicine, energy, ecology, and electronics. Due to electrical conductivity, tuneability, chemical stability, mechanical strength, and large surface area, over the years the number of its potential applications has increased. In this work, we prepared a derivate of graphene, and graphene oxide using two different methods, classical chemical oxidation of graphite using the modified Hummers method and electrochemical exfoliation of highly ordered pyrolytic graphite. Additionally, biochar was obtained using waste from fruit processing. Their structural properties have been investigated as well as their ability to block the propagation of electromagnetic waves in the low-frequency region (8-12 GHz).**

I. Introduction

Graphene is a single atomic layer of C atoms [1]. With the structure built strictly of sp^2 hybridized C atoms, it shows unique chemical, physical, optical, mechanical, and electrical properties [2, 3, 4, 5]. Namely, due to sp^2 hybridization of C atoms, graphene is highly hydrophobic, and repeals the water and other polar molecules [2]. Secondly, sp^2 hybridized C atoms are bonded into 6 members ring by conjugated bounds that are shorter and stronger compared to single sigma bonds, with a bond energy of 3.6-3.9 eV for C-C, compared to 4.93 eV in C-C bond in graphene [6]. Thanks to these bonds, graphene is one of the strongest materials with Young's module near 1 TPa [3]. Due to the delocalization of electrons from π orbitals, above and below C-C bonds, a unique cloud is created leading to another astonishing feature of graphene –a mobility of charge carrier of 10^6 cm^2 $V^{-1}s^{-1}$ [3].

Due to these outstanding properties, various techniques for graphene production have been developed over the last 20 years [7]. All methods are classified as bottom-up and top-down, depending if graphene is produced starting from molecules or is obtained from bulk material, respectively. Chemical vapor deposition, epitaxial growth of graphene on Si-C support, and thermal annealing often produce graphene with low defect number and high electrical conductivity [3]. However, these methods frequently limit the size of produced graphene to the size of the chamber, equipment is priced and demands the work of highly educated personnel, which all together increases the price of produced material. On the opposite, top-dawn methods more often lead to the production of graphene at a large scale but with a higher defect number.

One of the common top-down procedures to produce graphene is to oxidize graphite with strong oxidative agents and produce graphene oxide (GO), a derivate of graphene with various oxygen-containing functional groups. GO is not conductive due to discontinuity in π-cloud caused by functional groups or wholes in graphene sheets [7]. After chemical reduction, electrical properties are partially restored but not to the level of graphene which is why this type of graphene is called reduced graphene oxide (rGO) [8].

Another top-down technique transferable to large-scale production considering its simple experimental set-up, large yields and low consumption of chemicals is the electrochemical exfoliation of graphite [9].

In the past several years, the development of techniques where graphene-like materials are produced from different waste materials has attracted great attention as a sustainable alternative to graphene [10]. In the process of carbonization, many different sources of C atoms were turned into graphene, such as rice husk, olive stones, vegetables, fruits, and even insect parts [10].

In this work, we produced three different graphene-based nanomaterials: reduced graphene oxide (rGO), reduced electrochemical exfoliated graphene oxide obtained from highly oriented pyrolytic graphene (rHOPG), and graphene-like nanomaterial produced by pyrolysis of fruit biowaste. Raman, FTIR, and X-ray photoelectron spectroscopy (XPS) were used to investigate their structure while the shielding efficiency of materials was investigated with a vector network analyzer (VNA). Due to the emerging need for electromagnetic interference (EMI) shielding materials, increased attention is focused on nanostructured materials due to their exceptional characteristics such as a large specific surface area and ability to adsorb microwaves [11]. Carbon-based nanomaterials attracted great scientific attention as potential electromagnetic interference (EMI) shielding material due to lightweight, excellent electrical conductivity, resistance to humidity and various chemicals, elasticity, processability, durability, and environmental impact of synthetic approach [12, 13].

* This research supported by Horizon Europe Programme.

S. P. Jovanovic, M. Milenkovic and D. Kepic are with the Vinca Institute of Nuclear Sciences-National Institute of the Republic of Serbia, University of Belgrade, P.O. Box 522, 11000 Belgrade, Serbia; (corresponding author phone: +381 64 6143551; e-mail: svetlanajovanovic@vin.bg.ac.rs). M. Yasir and W. Saeed are with Carl von Ossietzky Universität Oldenburg, Oldenburg, Germany, I. Spanopoulos is with University of South Florida Tampa, FL, USA, Z. Syrgiannis is with Northwestern University, Evanston, Illinois, USA.

II. Experimental procedure

A. Synthesis of GO by modified Hummers

Graphite powder (1 g) was stirred with ccH_2SO_4 (23.3 mL) and $KMnO_4$ was slowly added (3 g) while the reaction mixture was held in the ice bath [11]. The mixture was stirred for 30 min. Then, the temperature was increased to 40 °C and stirred for 30 min, followed by the addition of 50 mL of water to the reaction mixture and heating at 95°C for 15 min. Then the reaction was stopped by pouring into water (150 mL) with 5 mL of H_2O_2 (30%). GO was cleaned using centrifugation (3500 rpm) and dialysis (MwCO 3500 kDa, for 7 days). In the end, water was removed by evaporation on reduced pressure and brown powder was collected.

The free-standing film was produced by vacuum filtration of 15 mL of GO water dispersion (concentration of 1 mg/mL). For reduction, films were immersed in a water solution of L-acrobic acid (15 mM) and HCl (0.017 mM) [12], and heated at 90 °C for 8 hours. After, the films were washed with water and dried at room temperature.

B. Synthesis of GO by electrochemical exfoliation of HOPG

To achieve electrochemical exfoliation, highly oriented pyrolytic graphite (HOPG, Vinca Institute of Nuclear Sciences, Serbia), an electrochemical cell with 2 electrodes (both the HOPG rods) was used and immersed in 0.1M water solution of ammonium persulfate which was served as an electrolyte. The distance between electrodes was 4 cm, and the applied direct current voltage was +12 V. Vacuum filtration was used to remove salt from exfoliated graphite. Then, exfoliated graphite was sonicated followed by centrifugation (at 3500 rpm) to remove large graphitic particles as precipitate. Both free-standing and reduced rHOPG were obtained as previously described for GO.

C. Synthesis of graphene-like material from a biowaste

Graphene-like material was produced in conventional pyrolysis of apple biowaste (stillage). Namely, the stillage was homogenized using the chopper, filtered, and dried. Then, obtained powder was mixed with the KOH in a mass ratio of 1:1, and heated at 850 °C for 1 hour. After, the obtained powder was washed with demineralized water. The resulting powder was used for analysis and named BA. In the laboratory conditions, to produce 1 g of carbonized materials it was needed around 3 working hours, while the price of produced materials is estimated to be around 1.2 euro per kg.

D. Structural analysis

To investigate the structure, FTIR spectroscopy was used. KBr powder and graphene samples were mixed and pastilles were obtained under press. Thermo Scientific Nicolet iS20 FTIR Spectrometer, Thermo Scientific™, Massachusetts, United States was used and it was operating in the range of 4000–400 cm^{-1} at 32 scans per spectrum.

DXR Raman microscope (Thermo Fisher Scientific, Waltham, MA, USA) was used to record Raman spectra, at room temperature. For excitation, a laser beam with a 532-nm wavelength was used. The power was 5 mW. The spectral resolution was 1 cm^{-1}, and the acquisition time was 10 × 10 s.

X-ray Photoelectron Spectroscopy (XPS) was performed using a Physical Electronics Industries PHI 5400 LS with a 10-360 Spherical Capacitor Analyzer (SCA). The SCA was set on aperture 2 small which yields an analysis area of 600 microns. The Aluminum K-alpha X-ray source was set to a power of 350 watts. SCA pass energy was set to 178.95 eV, with an eV/step of 0.250 eV. The samples were prepared by pressing the powder onto a substrate of Indium foil.

E. Microstrip-based characterization

A microstrip line-based prototype is required to characterize the BA. A prototype was fabricated using an LPKF micro-milling machine on Rogers RO4003C substrate with ε_r =3.38, tanδ=0.0027, thickness h=0.813 mm, and metal thickness t=35 µm. To obtain 50-Ω microstrip lines, a width of W=1.8 mm was adopted. The length of the gap is L=0.45 mm as shown in Fig. 1.

The measurement of S-parameters of the powdered BA sample was performed by converting it into a thin homogeneous film. To produce a thin film, a small amount of the BA sample was weighed on the digital weighing scale and then it was placed on a clean glass dish. A controlled amount of sodium silicate resin was added to the biomass sample using a micropipette until a homogeneous mixture was prepared. The amount of BA sample and sodium silicate used in the preparation was recorded. The complete method for preparing the biomass film is shown in Fig. 2. The concentration of the produced biomass film was 0.4083 g/mL. The film was deposited in the gap of the fabricated prototype evenly and then the prototype was placed on a hot plate.

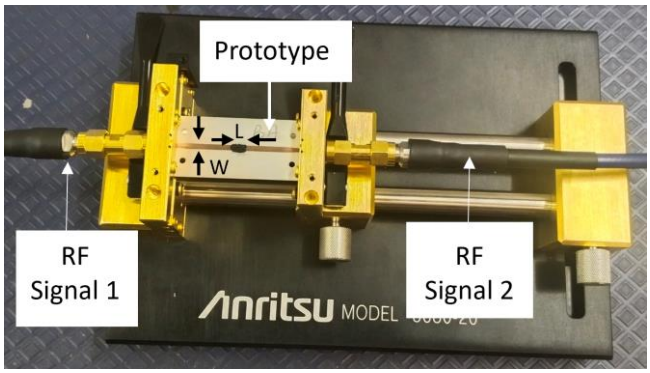

Figure 1. Microwave measurement set-up consisting of a VNA interfaced with Anritsu test fixture UTF 3680–20 with sample under test (SUT) to extract S-parameters.

The characterization setup for recording the S-parameters of the prepared film in the 8-12 GHz frequency band is shown in Fig. 1 which includes the ports of the VNA and the microstrip line with the film, all connected to the test fixture. The Anritsu test fixture UTF 3680-20 is used to connect the vector network analyzer ports (VNA) to the microstrip line. A thru-reflect-line calibration technique is used to exclude the impact of the microstrip lines from the transmission coefficient to get a precise value of S_{21} for the sample placed in the gap. The measured S_{21} is converted into complex impedance for further analysis of EM shielding.

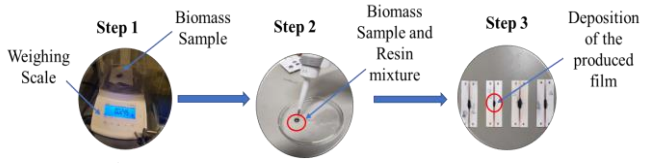

Figure 2. BA film preparation procedure.

F. Waveguide-based characterization

The S_{21} measurement of the rGO and rHOPG samples was carried out using the measurement setup shown in Fig. 3. The WR-90 waveguide adapters are connected to the VNA through VNA ports which provide the RF signal to the waveguide adapters. Thru-reflect-line calibration is used to precisely measure the S_{21} response of the sample under test which is placed between the two adapters in 8-12 GHz frequency band.

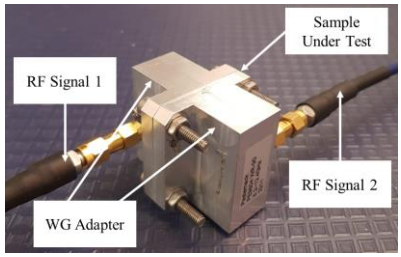

Figure 3. Microwave waveguide-based measurement set-up consisting of a VNA interfaced with WR-90 adapters with sample under test (SUT) sandwiched

III. RESULTS AND DISCUSSION

FTIR spectra of HOPG, BA, and GO are presented in Fig. 4. All spectra show strong bands around 3400 cm^{-1} which are assigned to OH groups or physically absorbed water [13]. It is noticeable that this band is higher in intensity in the case of GO and HOPG samples compared to BA where this band is very weak. The lower hydrophilic and lower number of OH functional groups in BA is probably the reason. Two weak bands at 2838 and 2929 cm^{-1} were observed in all three spectra and they stem from CH/CH_2, at 1730 cm^{-1} from C=O, at 1610 cm^{-1} C=C, at 1070 cm^{-1} from C-O [13]. These results indicated that all three materials contain sp^2 C atoms, CH/CH_2 groups, and oxygen-containing functional groups: carboxyl, hydroxyl, and carbonyl.

Raman spectra of HOPG, BA, and GO are presented in (Fig. 5). All spectra show D bend which is the result of the defect in the sp^2 graphene structure at 1351 cm^{-1}, and graphitic or so-called G shifting from 1596 to 1608 cm^{-1} [14]. The ratio between the integrated intensity of D and G bands is associated with structural disorder [14]. Disorder in graphene structure is related to the presence of O-containing functional groups and other defects such as vacancies, and sp^3 C atoms, in structure GO. The intensity ratio between G and D bands in the case of HOPG, BA, and GO are 0.82, 0.95, and 0.98, respectively. These results indicated that the highest structural order in the sample of HOPG indicated the largest content of C sp^2.

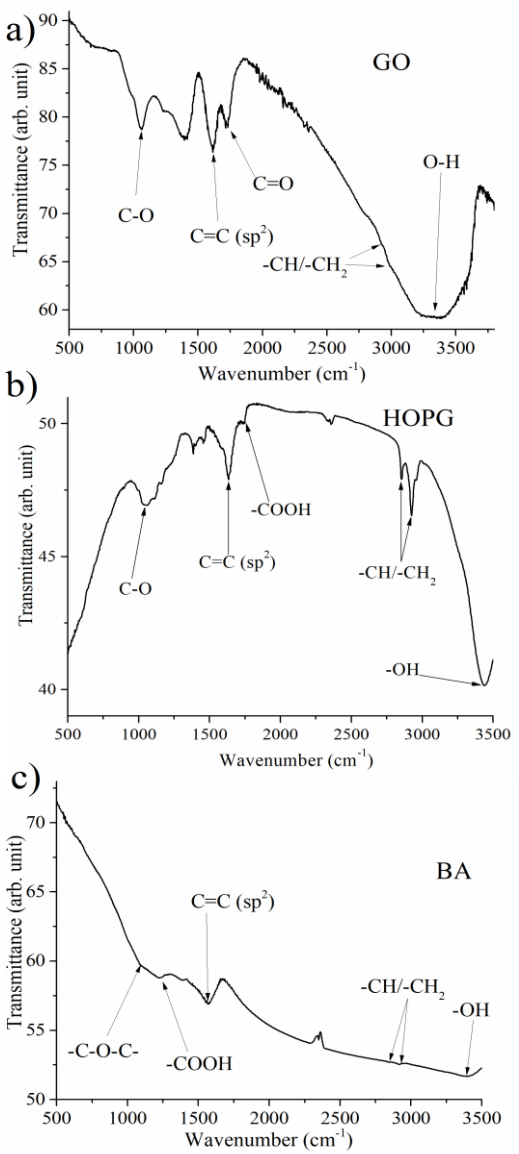

Figure 4. FTIR spectrum of GO (a), HOPG (b), and BA (c).

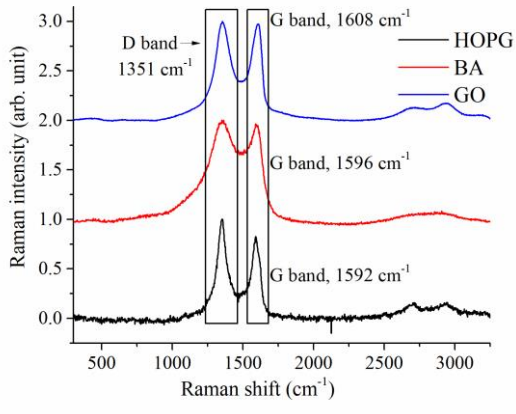

Figure 5. Raman spectra of HOPG, BA, and GO.

The structure of GO was investigated using XPS (Fig. 6). XPS survey spectra for all three samples show two main peaks, one from C1s at 283.4 eV and the second one at 528.6 eV from O1s [15]. In spectra of HOPG and GO peak at 346.7 eV was observed and assigned to N 1s. It was observed that material contains 61.34 at% of C and 38.66 at% O, while HOPG contains 54.20 at% of C and 34.31 at% O, and 3.3 at% of N, and BA only 34.51 at% of C and 65.01 at%. XPS analysis showed that the largest C content is in GO samples while the lowest at.% of C is in the sample of BA.

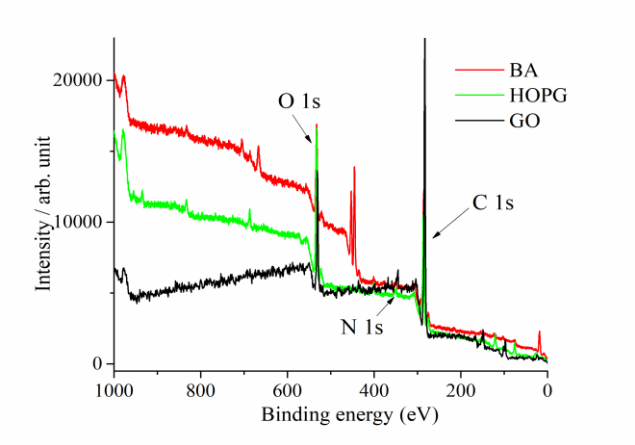

Figure 6. XPS survey spectra of BA, HOPG, and GO.

The measured S_{21} data for the BA sample was converted into complex impedance as shown in Fig. 7. The sample's complex impedance at a center frequency of 10 GHz was extracted and simulated in a commercially available EM simulation software, ANSYS HFSS. From the simulations, the attained S_{21} response corresponding to this complex impedance is shown in Fig. 8. It can be observed that 33.5% of the incident EM wave is reflected and 66.5% of the power is transmitted to port 2 of the VNA.

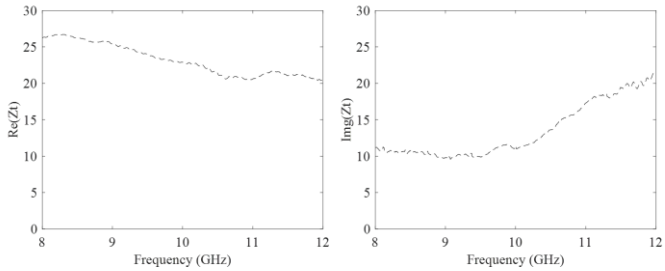

Figure 7. Complex impedance of biomass sample (a) resistance (b) reactance.

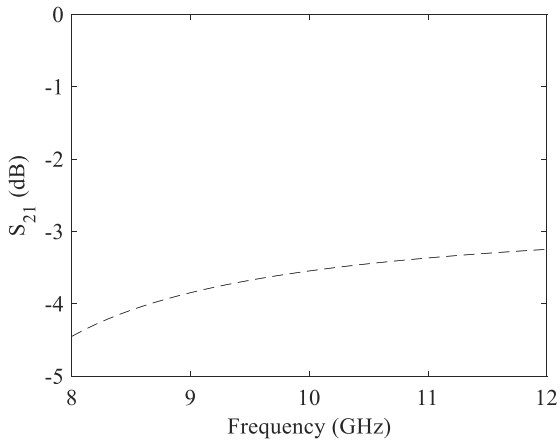

Figure 8. Simulated S_{21} response of the biomass sample.

By increasing the concentration of biomass sample 'BA' in the prepared film, a higher shielding can be achieved.

The measurement result for the rHOPG is shown in Fig. 9. The sample allows transmission of 91.4% of the incident wave whereas there is only an 8.6% reflection of the incident EM wave.

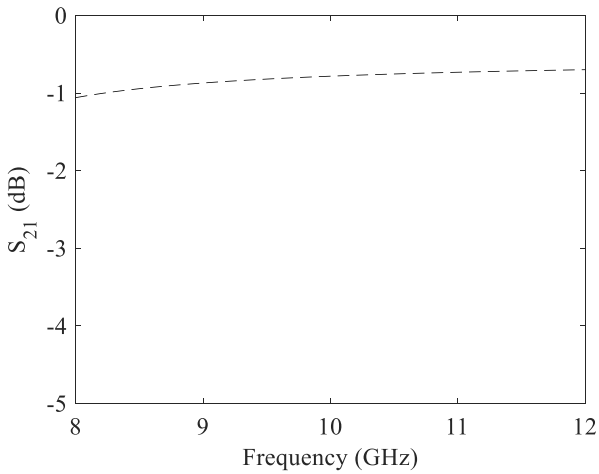

Figure 9. Measured S_{21} response of the rHOPG sample.

The measurement result for the rGO sample is shown in Fig. 10. The sample possesses the least shielding among the other two presented samples. Almost all the incident wave is transmitted from port 1 to port 2 of the VNA.

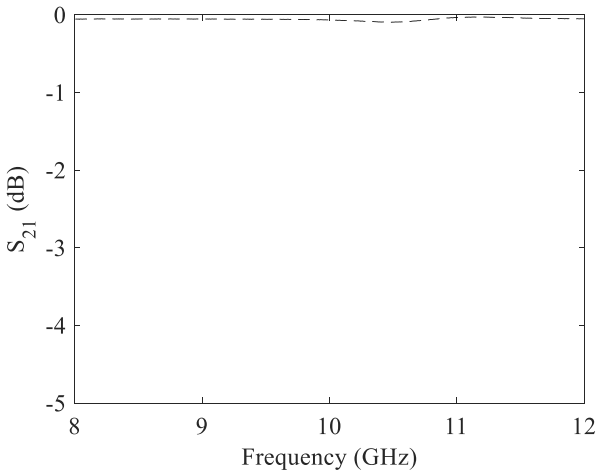

Figure 10. Measured S_{21} response of the rGO sample produced by Hummer's method.

IV. Conclusion

Producing the three different graphene-based nanomaterials, their structural properties were investigated using different spectroscopic techniques, Raman, FTIR, and XPS spectroscopy. These techniques showed that all samples containing sp^2 C in the structure as well as various oxygen-containing functional groups. The large structural disorder and the highest oxygen content were measured in the BA sample. The ability of produced materials to block the propagation of electromagnetic waves with the frequencies range between 8 and 12 GHz was investigated. The sample of rGO did not show any significant ability to block EMWs, while rHOPG was able to block only 8.6% of incident waves. But, in the case of BA, 33.5% of the incident EM wave was reflected indicating the ability of materials to block EMWs. The efficacy of shielding will be further improved by increasing the mass % of BA in composites. This is the first time according to the authors' best knowledge that the ability of stillage was used in the creation of EMW shielding material.

Acknowledgment

This research was funded by the European Union's Horizon Europe Coordination and Support Actions programme under grant agreement No 101079151 - GrInShield. S. J., M. M., D. K. thanks to the Ministry of Education, Science, and Technological Development of the Republic of Serbia (grant number 451-03-66/2024-03/ 200017).

References

[1] K. S. Novoselov, A. K. Geim, S. V. Morozov, D. Jiang, Y. Zhang, S. V. Dubonos, I. V. Grigorieva, A. A. Firsov, "Electric Field Effect in Atomically Thin Carbon Films", *Science*, vol. 306, 2004, pp. 666-669.

[2] A. R. Urade, I. Lahiri, K. S. Suresh, "Graphene Properties, Synthesis and Applications: A Review", *J.O.M*. 75, 2023, pp. 614-630.

[3] J. Prekodravac, D. Kepić, J. Carlos Colmenares, D. Giannakoudakis, S. Jovanović, "A comprehensive review on selected graphene synthesis methods: from electrochemical exfoliation through rapid thermal annealing towards biomass pyrolysis", *J. Mater. Chem. C*, vol. 9, 2021, pp. 6722-6748.

[4] Y. W. Sun, D. G. Papageorgiou, C. J. Humphreys, D. J. Dunstan, P. Puech, J. E. Proctor, C. Bousige, D. Machon, A. San-Miguel, "Mechanical properties of graphene", *Appl. Phys. Rev*. vol. 8 (2), 2021, pp. 021310.

[5] T. S. Sreeprasad, V. Berry, "How Do the Electrical Properties of Graphene Change with its Functionalization?", *Small*, vol. 9 (3), 2013, pp. 341–350.

[6] D. W. Brenner, O. A. Shenderova, J. A. Harrison, S. J. Stuart, B. Ni, S. B. Sinnott, "A second-generation reactive empirical bond order (REBO) potential energy expression for hydrocarbons", *J. Phys. Condens. Matt.*, vol. 14(4), 2002, pp. 783-802.

[7] A. Gutiérrez-Cruz, A. R. Ruiz-Hernández, J. F. Vega-Clemente, D. Guadalupe Luna-Gazcón, J. Campos-Delgado, "A review of top-down and bottom-up synthesis methods for the production of graphene, graphene oxide and reduced graphene oxide", *J. Mater. Sci*. vol. 57, 2022, pp. 14543-14578.

[8] J. Phiri, L. S. Johansson, P. Gane, T. Maloney, "A comparative study of mechanical, thermal and electrical properties of graphene-, graphene oxide- and reduced graphene oxide-doped microfibrillated cellulose nanocomposites", *Compos. B Eng.* vol. 147, 2018, pp. 104-113.

[9] F. Liu, C. Wang, X. Sui, M. A. Riaz, M. Xu, L. Wei, Y. Chen "Synthesis of graphene materials by electrochemical exfoliation: Recent progress and future potential", *Carbon Energy*. vol. 1, 2019, pp. 173-199.

[10] F. C. Asif, G. C. Saha, "Graphene-like Carbon Structure Synthesis from Biomass Pyrolysis: A Critical Review on Feedstock–Process–Properties Relationship", *C*, vol. 9, 2023, pp. 31.

[11] S. Zecchi, G. Cristoforo, M. Bartoli, A. Tagliaferro, D. Torsello, C. Rosso, M. Boccaccio, F. Acerra, "A Comprehensive Review of Electromagnetic Interference Shielding Composite Materials", *Micromachines*, vol. 15, 2024, pp. 187.

[12] S. Jovanović, M. Huskić, D. Kepić, M. Yasir, K. Haddadi, "A review on graphene and graphene composites for application in electromagnetic shielding", *Graphene and 2D mater*, vol. 8, 2023, pp. 59-80.

[13] P. Savi, M. Yasir, "Waveguide measurements of biochar derived from sewage sludge". *Electron. Lett*., vol. 56, 2020, pp. 335-337.

[14] J. Chen, B. Yao, C. Li, G. Shi, "An improved Hummers method for eco-friendly synthesis of graphene oxide", *Carbon*, vol. 64, 2013, pp. 225-229.

[15] M. J. Fernández-Merino, L. Guardia, J. I. Paredes, S. Villar-Rodil, P. Solís-Fernández, A. Martínez-Alonso, J. M. D. Tascón, "Vitamin C Is an Ideal Substitute for Hydrazine in the Reduction of Graphene Oxide Suspensions", *J. Phys. Chem. C*, vol. 114, 2010, pp. 6426-6432.

[16] I. O. Faniyi, O. Fasakin, B. Olofinjana, A. S. Adekunle, T. V. Oluwasusi, M. A. Eleruja, E. O. B. Ajayi, "The comparative analyses of reduced graphene oxide (RGO) prepared via green, mild and chemical approaches", *SN Appl. Sci.* vol. 1, 2019, pp. 1181.

[17] J. B. Wu, M. L. Lin, X. Cong, H. N. Liua, P. H. Tan, "Raman spectroscopy of graphene-based materials and its applications in related devices", *Chem. Soc. Rev*., vol. 47, 2018, pp.1822-1873.

[18] F. H. Wang, K. Bae, Z. W. Huang, J. M. Xue, "Two-photon graphene quantum dot modified Gd2O3 nanocomposites as a dual-mode MRI contrast agent and cell labelling agent", *Nanoscale*, vol. 10, 2018, pp. 5642-5649.